POWER SYSTEMS AND POWER ELECTRONICS

# Research on collaborative optimization of fuel cell tractor transmission system and control strategy parameters

Liyou XU[1,2], Shixun CHEN[1], Junjiang ZHANG[1,2]*, Mengnan LIU[3], Yiwei WU[1,2], and Xianghai YAN[1,2]

[1] College of Vehicle and Traffic Engineering, Henan University of Science and Technology, Luoyang 471003, China
[2] State Key Laboratory of Intelligent Agricultural Power Equipment, Luoyang 471039, China
[3] YTO Group Corporation, Luoyang 471004, China

**Abstract.** The distributed fuel cell tractor is a new type of power tractor. The transmission system and control strategy parameters affect the energy utilization efficiency of the entire machine. There is currently no research in this area. In order to solve the problem of low energy utilization of the whole machine of distributed dual-motor-driven hydrogen fuel cell tractor, a cooperative optimization method is proposed, based on particle swarm optimization (PSO) algorithm for the parameters of the transmission system and energy-saving control strategy of distributed dual-motor-driven hydrogen fuel cell tractor. According to the tractor dynamics analysis and equivalent hydrogen consumption theory, a fuel cell tractor transmission parameter-equivalent hydrogen consumption model is established, The wheel-side transmission ratio and the upper and lower threshold values of the hydrogen fuel cell working power are taken as control variables, and the minimum equivalent hydrogen consumption is taken as the optimization goal, the optimization method is simulated and tested based on the MATLAB simulation platform. The results show that under plowing conditions, compared with the rule-based control strategy, the proposed collaborative optimization method of the fuel cell tractor transmission system and control strategy parameters can reasonably control the operating status of the fuel cell and the power battery, ensure that the fuel cell works in a high-efficiency range, enhance the overall performance of the fuel cell system, and control the power battery state of charge (SOC) to remain in a reasonable range. The tractor equivalent hydrogen consumption is reduced by 7.84%.

**Keywords:** hydrogen fuel cell; electric tractor; parameter optimization; energy-saving control.

## 1. INTRODUCTION

The progress of the modern agricultural industry and a new production mode impose higher standards on production efficiency and emission reduction. As an important energy-consuming field, agricultural equipment, intelligent agricultural machinery equipment based on new energy has become an important direction for the green transformation and upgrading of agricultural production machinery in the future due to its good mechanical design characteristics and clean and low pollution [1–5]. Among them, fuel cells are ideal conversion devices for green and low-carbon hydrogen energy, which is abundant. Since they do not go through the thermal engine process, the energy conversion rate is as high as 40%–60%, but they have the characteristics of soft output characteristics and slow dynamic response. They are usually equipped with auxiliary power sources such as power batteries to adapt to the complex operating environment of tractors [6, 7].

Transmission system parameters and energy management strategies are two important ways to improve the energy utilization of tractors. The optimization of transmission system parameters mainly uses the output characteristics of the motor

or internal combustion engine to make it work in the high-efficiency zone as much as possible. At present, a lot of research is conducted in this area. In the paper [8], a parameter matching and optimization design method for the electric tractor powertrain based on the dual-motor coupling drive mode was proposed, among others. The particle swarm optimization algorithm based on the hybrid penalty function was used for parameter optimization, which improved the traction performance of the electric tractor. However, the output power of the main motor and the auxiliary motor was not optimized to reduce energy consumption. In the paper [9], after multi-objective optimization of the transmission system parameters under urban conditions using a multi-island genetic algorithm, the fuel consumption of the hybrid bus was reduced by 11.6%, but the parameters of the rule-based energy management strategy were not optimized. In the paper [10], a transmission speed ratio optimization method based on the life cycle speed utilization of a general agricultural tractor was proposed. The multi-speed power shift transmission of an agricultural tractor was taken as the research object, and a genetic algorithm was used to optimize the speed ratio parameters. This method can significantly improve fuel economy. However, it is aimed at traditional tractors and does not consider the power optimization problem among multiple power sources. In the paper [10], a transmission speed ratio optimization method based on the life cycle speed utilization of a general agricultural tractor was proposed. The multi-speed power shift transmission

*Bull. Pol. Acad. Sci. Tech. Sci.*, vol. 73, no. 2, p. e153232, 2025

1

L. Xu, S. Chen, J. Zhang, M. Liu, Y. Wu, and X. Yan

of an agricultural tractor was taken as the research object, and a genetic algorithm was used to optimize the speed ratio parameters. This method can significantly improve fuel economy. However, it is aimed at traditional tractors and does not consider the power optimization problem among multiple power sources. In the paper [11], a front and rear wheel transmission ratio parameter optimization strategy based on a multi-island genetic algorithm was proposed. Under the plowing cycle condition, the performance of the distributed drive system in all aspects was effectively improved, but the power distribution optimization problem among multiple energy sources was not considered. In the paper [12], a parametric collaborative optimization design method considering the drive system and the energy system was proposed. The front and rear wheel transmission ratio was optimized based on the multi-island genetic algorithm, and the global optimal power distribution ratio was found based on the dynamic programming algorithm. The total energy consumption was reduced by 15.39%. Although the collaborative optimization of parameter optimization and energy management strategy was considered, the parameters of the control strategy were not optimized. It can be seen that the transmission system parameters have a profound influence on the energy efficiency of the whole machine. Although the above scholars conducted fruitful research, they did not consider the impact of the control strategy parameters on the energy efficiency of the whole machine.

Energy management optimization for multiple energy sources or multiple power sources can also reduce the energy consumption of the entire machine. In the paper [13], based on the powertrain modelling of fuel cell electric vehicles, the framework construction and parameter update process of the energy management algorithm based on reinforcement learning were completed, and it was applied to fuel cell electric vehicles. The simulation and experimental results show that the proposed algorithm can minimize hydrogen consumption and maintain the battery SOC stable but it does not optimize the transmission system parameters. In the paper [14], a multi-layer decoupling control energy management strategy based on Haar wavelet and logic rules was designed. The results showed that compared with single-layer control strategies such as fuzzy control and power tracking control, the multi-layer control strategy can more reasonably allocate the required power. The average efficiency of hydrogen fuel cells was increased by 2.87% and 1.2%, respectively, but the transmission system parameters were not optimized. In the paper [15], a controllable neural model for fuel cell vehicle energy management is proposed, with better fuel economy compared with the adaptive equivalent consumption minimization strategy, but the transmission system parameters are not optimized. In the paper [16], a mileage-adaptive equivalent hydrogen consumption minimization strategy was developed that integrated the operating condition prediction. The hydrogen consumption under the urban road cycle condition was 55.6% lower than that of the power consumption maintenance strategy, and the hydrogen consumption under the suburban cycle condition was reduced by 26.8%. Although the operating conditions were predicted, no further consideration was given to optimizing the transmission system parameters according to the operating conditions to reduce hydrogen consumption. In the paper [17], the proposed improved equivalent hydrogen consumption algorithm can realize the energy distribution of the hybrid system under complex working conditions. The added voltage balance coefficient can ensure that the voltage of the supercapacitor at the end of the vehicle interval is within a reasonable range, but the influence of the transmission system parameters is not considered. The aforementioned scholars conducted a lot of research on control strategies and achieved satisfactory results, but they did not consider the impact of transmission system parameters on the energy utilization efficiency of the whole machine.

In summary, both the transmission system parameters and the control strategy parameters greatly impact the energy utilization efficiency of the whole machine. However, there are few reports on the collaborative optimization of the two. In order to improve the energy utilization efficiency of distributed dual-motor driven hydrogen fuel cell tractors, this paper proposes a collaborative optimization method of transmission system and control strategy parameters. This paper is organized as follows: the first part is an introduction. The second part presents the topological structure, power system model, and instantaneous equivalent hydrogen consumption model of the distributed dual-motor driven hydrogen fuel cell tractor. The third part introduces the collaborative optimization method of the transmission system and control strategy parameters, and the rule-based comparison method proposed in this paper. The fourth part compares and analyzes the simulation results under different strategies. The fifth part gives the conclusion.

## 2. TRACTOR POWER STRUCTURE AND MODEL BUILDING

### 2.1. Fuel cell tractor topology and main component performance parameters

The structure of the distributed dual-motor driven hydrogen fuel cell tractor is shown in Fig. 1. The tractor has two energy sources: fuel cells and power batteries. The output torque of the wheel-
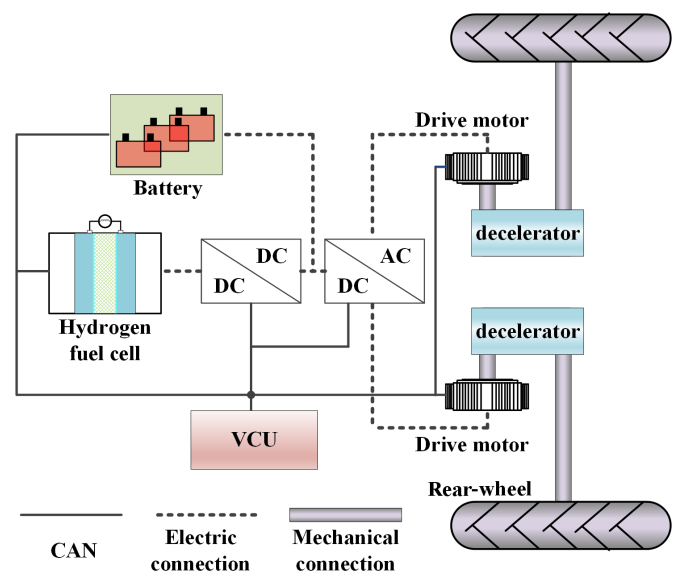


**Fig. 1.** Topological structure of fuel cell tractor

2

*Bull. Pol. Acad. Sci. Tech. Sci.*, vol. 73, no. 2, p. e153232, 2025

side motor is directly transmitted to the drive wheel through the reducer. The fuel cell, power battery, DC/DC module, DC/AC module, and two-wheel-side drive motors are connected to the vehicle controller through the controller area network (CAN) bus. The vehicle controller dynamically allocates the output power of the fuel cell and power battery according to the energy management strategy based on the total power demand of the whole machine and the SOC state of the power battery, so that the tractor can obtain the best power and economy.

This paper contains an analysis of a certain type of fuel cell tractor, whose main technical parameters are shown in Table 1.

**Table 1**

Main parameters of tractor

| Item | Parameters/units | Value |
|------|------------------|-------|
| Vehicle parameters | Tractor usage quality/kg | 2500 |
| | Rolling radius of driving wheel/m | 0.63 |
| | Rolling resistance coefficient | 0.07 |
| | Speed ratio of reducer | 33 |
| Drive motor | Rated speed/r·min$^{-1}$ | 1500 |
| | Rated torque/N·m | 140 |
| | Rated power/kW | 22 |
| | Maximum speed/r·min$^{-1}$ | 3000 |
| Battery | Energy capacity/A·h | 40 |
| | Rated voltage/V | 380 |
| Fuel cell | Peak power/kW | 45 |

## 2.2. Tractor dynamics model

The power required by hydrogen fuel cell hybrid tractors comes from hydrogen fuel cells and power batteries. The input terminals of the dual motors are used to calculate the required power of the whole machine, which is expressed by the following formula:

$$P_{\text{req}} = \left(P_{fc}\eta_{DD} + P_{\text{bat}}\right)\eta_{DA}, \tag{1}$$

where $P_{fc}$ represents the fuel cell output power, in kW; $\eta_{DD}$ represents the efficiency of the DC/DC converter, %; $P_{\text{bat}}$ represents the instantaneous power of the power battery, in kW; $\eta_{DA}$ represents the DC/AC converter efficiency, %.

The paper focuses on the plowing working conditions of tractors as a common working condition. It analyzes the driving force and driving resistance of the tractor. When the tractor is running, the driving force should be equal to the sum of the driving resistances. At the same time, when the tractor is plowing in the field, the main driving resistance comes from the traction resistance that must be overcome by pulling the agricultural implements [18, 19]. Since the tractor travels at a slow speed under plowing conditions, air resistance is generally ignored. Therefore, the driving equation of the plowing tractor is:

$$F_t = mgf + F_{TN}, \tag{2}$$

where $F_t$ represents the driving force of the whole machine, in kN; $m$ represents the tractor usage quality, in kg; $g$ represents the acceleration due to gravity, which is 9.8 m/s$^2$; $f$ represents the rolling resistance coefficient; $F_{TN}$ represents the plowing resistance, in kN.

Also, $F_{TN}$ is determined by the matching agricultural machinery and can be shown as:

$$F_{TN} = zb_l h_k k, \tag{3}$$

where $z$ represents the number of plowshares, which is 3; $b_l$ represents the width of a single plowshare, which is 20 cm; $h_k$ represents the depth of plowing, in centimetres; $k$ represents the soil specific resistance, which is 7 N/cm.

Combining formulas (2) and (3), the sum of the required power at the input ends of the tractor dual motors under plowing conditions is as follows:

$$P_{\text{req}} = \frac{F_t v}{3.6\eta_r \eta_m}, \tag{4}$$

where $v$ represents the tractor driving speed, in km/h; $\eta_r$ represents the transmission efficiency of the reducer, which is 0.95; $\eta_m$ represents the efficiency of the drive motor.

To calculate the output speed of the motor according to the tractor's driving speed and the parameters of the reducer:

$$n_m = \frac{vi}{0.377r}, \tag{5}$$

where $n_m$ represents the output speed of the drive motor, in r/min; $i$ represents the speed ratio of the reducer; $r$ represents the radius of the driving wheel, in metres.

Combining formulas (4) and (5), the output torque of the motor can be obtained:

$$T_m = \frac{9550F_t v}{7.2\eta_r n_m}. \tag{6}$$

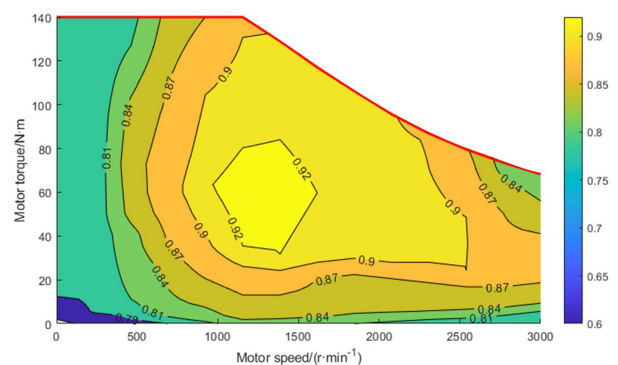Thus, we obtain the efficiency of the motor by interpolation in Fig. 2.



**Fig. 2.** Drive motor MAP diagram

## 2.3. Hydrogen fuel cell system model construction

The hydrogen fuel cell system model mainly includes hydrogen fuel cells and power batteries. The high energy density of hydrogen fuel cells can provide a higher endurance for the whole

L. Xu, S. Chen, J. Zhang, M. Liu, Y. Wu, and X. Yan

machine operation, while the power battery can provide high power in a brief time, which is suitable for high load requirements. The combination of the two forms a hybrid power system, which can maximize the clean characteristics of hydrogen energy and extend the service life of hydrogen fuel cells [20]. The fuel cell operation characteristics used in this paper are shown in Fig. 3.
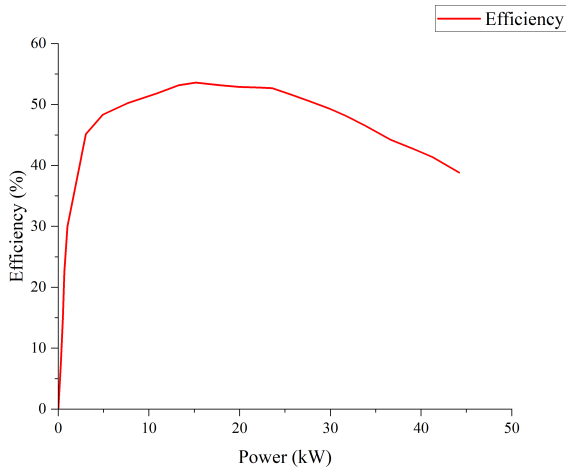


**Fig. 3.** Fuel cell operating characteristics diagram

Common battery models include the internal resistance model, first-order RC model, and neural network model. The battery model established in this paper is an equivalent internal resistance model with a voltage source and internal resistance [21–23], as shown in Fig. 4.
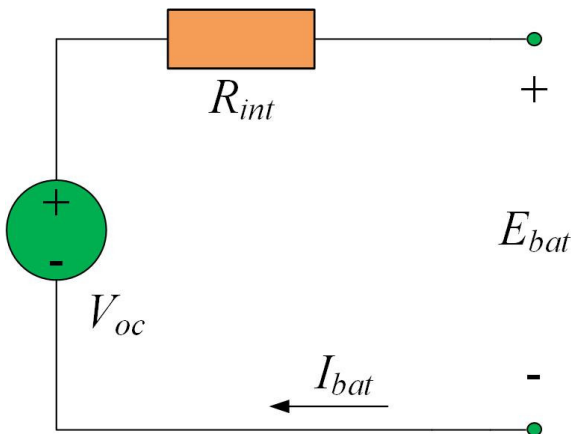


**Fig. 4.** Equivalent internal resistance model

The output power $P_{bat}$ of the battery is related to the open circuit voltage, current and internal resistance of the battery, which can be expressed as follows:

$$P_{bat} = V_{oc}(SOC)I_{bat} - I_{bat}^2 R_{int}(SOC), \qquad (7)$$

where $V_{oc}(SOC)$ represents the open circuit voltage of the battery, related to the SOC of the battery, in V; $I_{bat}$ represents the battery current, in A; $R_{int}(SOC)$ represents the internal resistance of the battery, related to the SOC of the battery, in Ω.

The relationship curve between battery electromotive force, charge and discharge internal resistance $R_{int}$ and battery SOC is shown in Fig. 5.
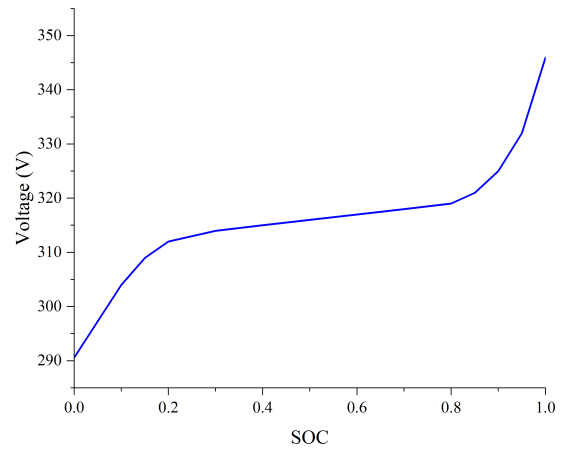


(a) Relationship between electromotive force and SOC
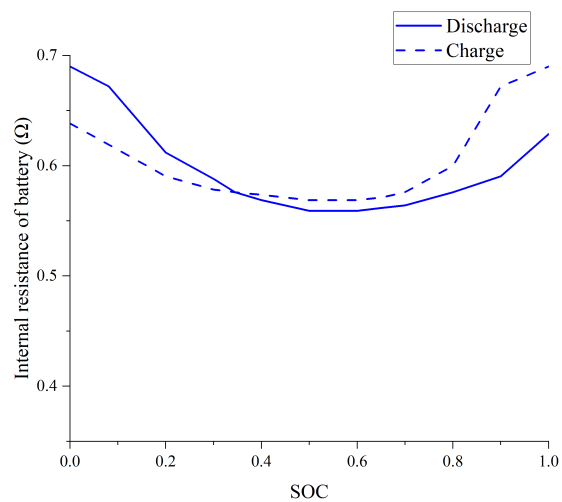


(b) Relationship between charge and discharge internal resistance and SOC

**Fig. 5.** Relationship between electromotive force, battery charge and discharge internal resistance and battery SOC

Combined with formula (7), the instantaneous charge and discharge efficiency of the battery can be expressed as:

$$\begin{cases} \eta_{dis} = \dfrac{1 + \sqrt{1 - \dfrac{4R_{int}P_{bat}(t)}{V_{oc}^2}}}{2}, & P_{bat} \geq 0, \\[4mm] \eta_{chg} = \dfrac{2}{1 + \sqrt{1 - \dfrac{4R_{int}P_{bat}(t)}{V_{oc}^2}}}, & P_{bat} < 0, \end{cases} \qquad (8)$$

where $\eta_{dis}$ represents the discharge efficiency of the battery; $\eta_{chg}$ represents the charging efficiency of the battery.

This paper uses the ampere-hour integration method to calculate the battery SOC, the formula is as follows:

$$SOC(t) = SOC(0) - \frac{\int_0^t I_{\text{bat}}(t)\,dt}{Q_{\text{bat}}}, \tag{9}$$

where $SOC(0)$ represents the initial SOC of the battery, %; $Q_{bat}$ represents the rated capacity of the battery, in A·h.

## 2.4. Instantaneous equivalent hydrogen consumption model of the system

Equivalent hydrogen consumption theory, as a theory used to evaluate hydrogen consumption in different energy source systems, plays a significant role in the design optimization of fuel cell hybrid systems. In this paper, the equivalent hydrogen consumption model formula of the system [24–27], is expressed as follows:

$$C_{\text{sys}} = C_{fc} + C_{\text{bat}}. \tag{10}$$

Then, $C_{fc}$ represents the hydrogen consumption of the fuel cell and can be expressed as follows:

$$C_{fc} = \frac{P_{fc}}{E_{\text{H}_2,\text{low}}\,\eta_{fc}\left(P_{fc}\right)}, \tag{11}$$

where $E_{\text{H}_2,\text{low}}$ represents the lower calorific value of hydrogen, which is 120 kJ/g; $\eta_{fc}$ represents the discharge efficiency of the fuel cell.

The equivalent hydrogen consumption $C_{\text{bat}}$ when the power battery is charged/discharged is:

$$C_{\text{bat}} = \begin{cases} \dfrac{P_{\text{bat}}}{E_{\text{H}_2,\text{low}}\,\overline{\eta}_{fc}\,\eta_{\text{dis}}}, & P_{\text{bat}} \geq 0, \\[3mm] \dfrac{P_{\text{bat}}\,\eta_{chg}}{E_{\text{H}_2,\text{low}}\,\overline{\eta}_{fc}}, & P_{\text{bat}} < 0, \end{cases} \tag{12}$$

where $\overline{\eta}_{fc}$ represents the average discharge efficiency of the fuel cell.

## 3. ENERGY MANAGEMENT STRATEGY DESIGN

The overall goal of energy system power optimization is to improve the fuel utilization efficiency of the entire machine based on meeting the power required by the tractor load. Combined with the output characteristics of the fuel cell and power battery, to avoid frequent starts and stops affecting battery performance [28,29], set the minimum stable output power $P_{\min}$ of the fuel cell. To ensure that the fuel cell works in the high-efficiency range, the maximum output power $P_{\max}$ of the fuel cell is set. At the same time, due to the slow dynamic response of the fuel cell and frequent load changes, the battery life is reduced. Try to ensure that the output power of the fuel cell is within a certain range. As concerns internal fluctuations, the SOC of the power battery is maintained at [30%, 90%] to avoid sudden drops and rises in battery voltage, which may cause over-discharge and overcharge of the battery, and to ensure the power performance of the vehicle.

## 3.1. Collaborative optimization of fuel cell tractor transmission system parameters and control strategies

### 3.1.1. Hydrogen fuel cell system power optimization

This paper takes the minimum equivalent hydrogen consumption of the system as the objective function. When optimizing the system power, to maintain the health of the power battery, extend its service life, and ensure that the SOC of the power battery is within a reasonable range, a power battery charge retention strategy is introduced [30], with the following formula:

$$\alpha(SOC) = 1 - \beta\left(\frac{2SOC - (SOC_H + SOC_L)}{(SOC_H - SOC_L)}\right), \tag{13}$$

where $SOC_H = 0.9$; $SOC_L = 0.3$; $\beta$ is the adjustment coefficient. By calibrating $\beta$, the power battery SOC can be effectively kept within a reasonable range. After calibration, $\beta = 0.5$.

After modification, the optimization objective function of the system equivalent hydrogen consumption is:

$$\min\left(C_{\text{sys}}\right) = \min\left(C_{fc} + \alpha(SOC)C_{\text{bat}}\right). \tag{14}$$

At the same time, since the power optimization of the tractor hydrogen fuel cell system is constrained by the working capacity of each component, the parameters in Fig. 6 must satisfy the
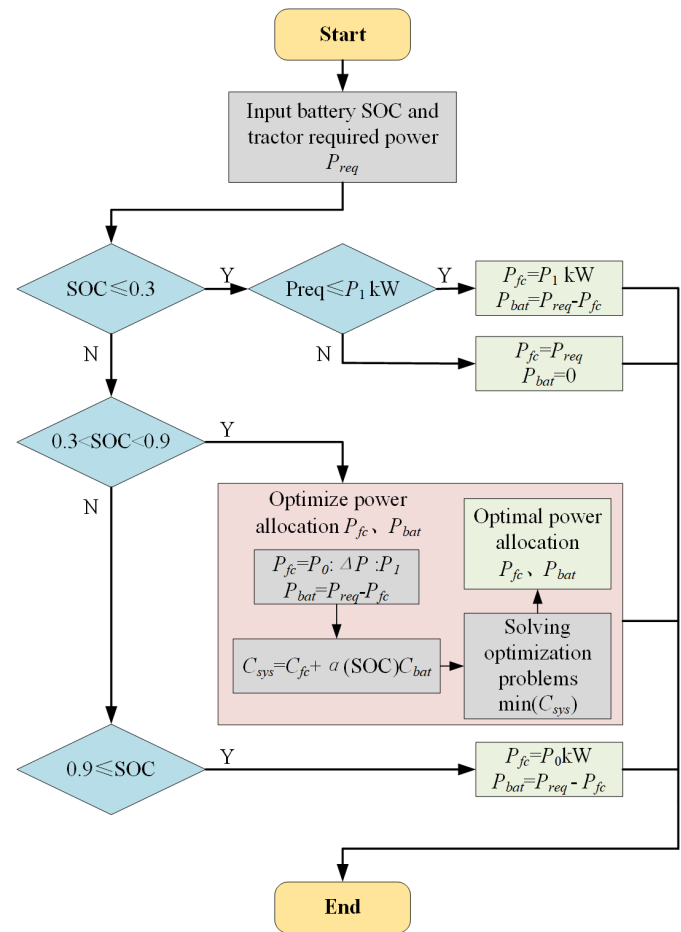


**Fig. 6.** Power optimization flowchart

*Bull. Pol. Acad. Sci. Tech. Sci.*, vol. 73, no. 2, p. e153232, 2025

5

L. Xu, S. Chen, J. Zhang, M. Liu, Y. Wu, and X. Yan

constraint condition (15).

$$\begin{cases} P_{\min} \leq P_0 \leq P_1 \leq P_{\max} \leq P_{\text{peak}}, \\ P_{ch\max} \leq P_{\text{bat}} \leq P_{\text{dis}\max}, \end{cases} \qquad (15)$$

where $P_0$ and $P_1$ represent the minimum stable output power and maximum output power of the fuel cell, respectively, and are the parameters to be optimized in Fig. 6; $P_{\text{peak}}$ represents the peak power of the fuel cell; $P_{ch\max}$ represents the maximum charging power of the power battery, which is a negative value; $P_{\text{dis}\max}$ represents the maximum discharge power of the power battery, which is a positive value.

### 3.1.2. PSO parameters optimization

The particle swarm algorithm is one of the most famous population-based optimization techniques inspired by nature. Its advantages are strong global optimization ability and fast convergence speed [31–33]. In each iteration, the particle swarm algorithm continuously changes its speed and position by tracking individual extreme values and population extreme values. Its speed and position can be expressed as:

$$\begin{cases} v_i^{t+1} = \omega(t) v_i^t + c_1 r_1 (p_i^t - x_i^t) + c_2 r_2 (p_{Gi}^t - x_i^t), \\ x_i^{t+1} = x_i^t + v_i^{t+1}, \end{cases} \qquad (16)$$

where $\omega(t)$ is the inertia weight; $c_1$, $c_2$ is the learning factor; $r_1$ and $r_2$ are random numbers in the range $[0,1]$; $v_i^t$ and $v_i^{t+1}$ are the velocities of particle $i$ at time $t$ and $t+1$, respectively; $x_i^t$ and $x_i^{t+1}$ are the positions of particle $i$ at time $t$ and $t+1$ respectively; $p_i^t$ and $p_{Gi}^t$ are the optimal solutions for the individual and the population respectively within time $t$; $i = 1, 2, \ldots, d$.

Based on the multi-objective optimization of PSO parameters, the wheel reducer ratio i, the minimum stable power p0 of the hydrogen fuel cell, and the maximum output power p1 of the fuel cell are selected as the three-dimensional position coordinates of the particles, and the equivalent hydrogen consumption is the population fitness. The specific steps for the coordinated optimization of the transmission system and control strategy parameters are as follows:

(a) The population size of the particle swarm algorithm is initialized at 3, the maximum number of iterations is 150, the inertia weight is 0.9, the learning factor is 0.5, the space dimension is 3, the three dimensions represent $i$, $P_0$, $P_1$ and the particle ranges are $30, 45]$, $[5, 16]$, $[16, 30]$, respectively.
(b) To calculate the fitness of all particles (equivalent hydrogen consumption), input the particle parameters, transmission system and control strategy parameters, and specific operating conditions information into the energy system power optimization module.
(c) Update individual optimal $p_i^t$ and global optimal $p_{Gi}^t$.
(d) The particle position and search speed are updated through equation (16).
(e) Determine whether the number of iterations reaches the maximum number of iterations, i.e., 150. If it does not reach the maximum number of iterations, repeat steps (b), (c), and (d) until the judgment conditions are met and output the historical best particle position.

The optimization process is shown in Fig. 7. The power optimization module in the flow chart uses the process demonstrated in Fig. 6 mentioned before.
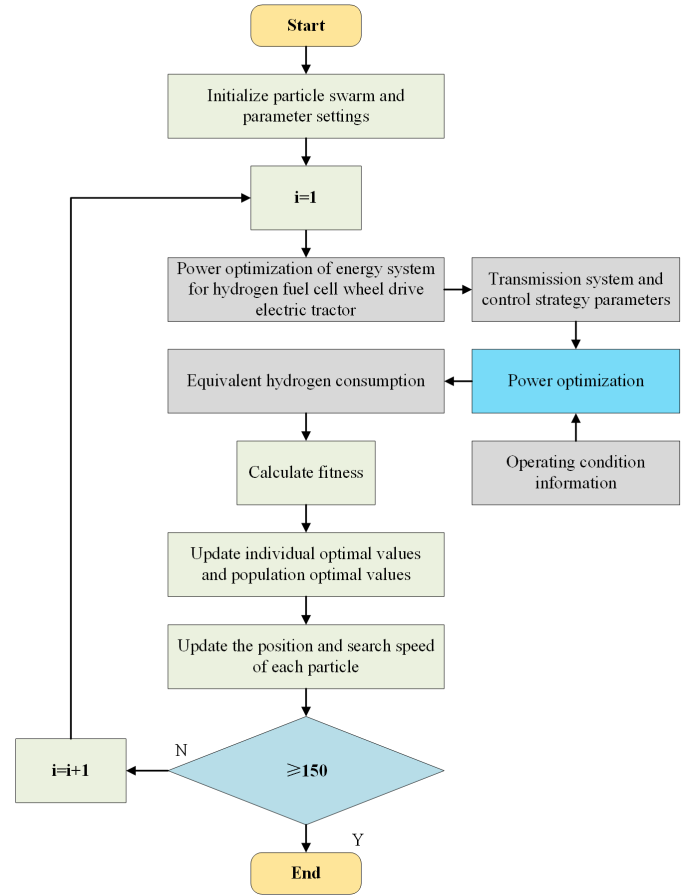


**Fig. 7.** Optimization flow chart based on PSO

### 3.2. Rule-based control strategy

This paper adopts a rule-based control strategy as a comparative method. In the hydrogen fuel cell system, due to the high charging and discharging efficiency of the power battery, the power battery is used as the main energy source and the hydrogen fuel cell is used as the auxiliary energy source. Therefore, according to the relationship between the power battery SOC value, the maximum charging power $P_{ch\max}$, the maximum discharge power $P_{dismax}$, and the tractor demand power $P_{\text{req}}$, the following strategy is formulated to allocate the required power to the two power sources of the fuel cell and the power battery. The mode rules are shown in Table 2.

If the initial state of the power battery SOC is less than or equal to 0.3, the power distribution is controlled according to Mode B until the SOC rises to 0.9 and then changes to Mode A, and when the SOC drops to 0.3, it changes to Mode B, and so on.

If the initial state of the power battery SOC is greater than 0.3, the power distribution is controlled according to Mode A until the SOC drops to 0.3 and then changes to Mode B, and when the SOC rises to 0.9, it changes to Mode A, etc.

6

*Bull. Pol. Acad. Sci. Tech. Sci.*, vol. 73, no. 2, p. e153232, 2025

**Table 2**
Mode rules

| Mode | State | Power demand $P_{req}$ | Power allocation |
|------|-------|------------------------|------------------|
| A | 1 | $P_{req} > P_{dis\,max} + P_{min}$ | $P_{fc} = P_{req} - P_{dis\,max}$<br>$P_{bat} = P_{dis\,max}$ |
| A | 2 | $P_{req} \leq P_{dis\,max} + P_{min}$ | $P_{fc} = P_{min}$<br>$P_{bat} = P_{req} - P_{min}$ |
| B | 1 | $P_{req} \geq P_{ch\,max} + P_{max}$ | $P_{fc} = P_{max}$<br>$P_{bat} = P_{req} - P_{max}$ |
| B | 2 | $P_{req} < P_{ch\,max} + P_{max}$ | $P_{fc} = P_{req} - P_{ch\,max}$<br>$P_{bat} = P_{ch\,max}$ |
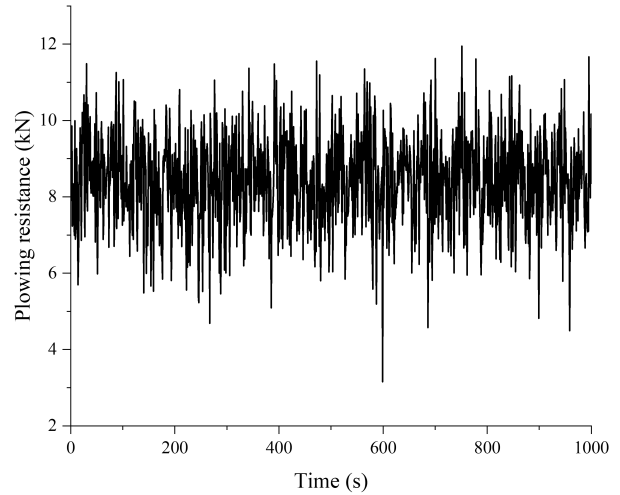
## 4. ANALYSIS OF RESULTS

The plowing condition is selected as the tractor simulation condition, and the initial state of the power battery SOC is set to 0.5. Under plowing conditions, the driving speed and traction resistance of the tractor will change accordingly because it is affected by soil conditions, the tractor performance, driver operation, and external environment. The tractor travel speed is shown in Fig. 8. The travel speed fluctuates at 7 km/h, with a maximum speed of 9.78 km/h and a minimum speed of 4.12 km/h. The plowing resistance is shown in Fig. 9. The plowing resistance fluctuates at 8.5 kN, with the highest resistance reaching 11.96 kN and the lowest resistance reaching 3.15 kN.
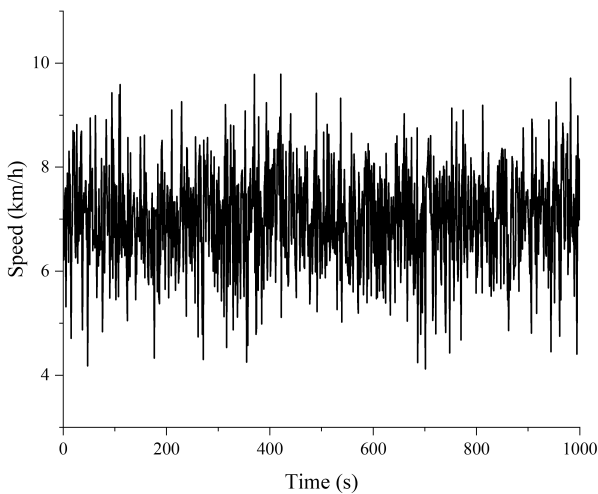


**Fig. 8.** Plowing speed

Under the plowing simulation condition, Table 3 shows the comparison of the hydrogen fuel cell tractor parameters before and after optimization. The optimized parameters are the particle positions corresponding to the minimum particle fitness under the collaborative optimization control strategy.

Figure 10 shows the fitness of the particle swarm algorithm. The smaller the fitness value, the better the solution corresponding to the particle. As can be seen from the figure, the fitness converges quickly after 75 generations and finally converges to



**Fig. 9.** Plowing resistance

**Table 3**
Comparison of hydrogen fuel cell tractor parameters before and after optimization

| Item | Before optimization | After optimization |
|------|---------------------|--------------------|
| Speed ratio of reducer | 33 | 42.6274 |
| Minimum output power of fuel cell/kW | 8 | 14.9821 |
| Maximum output power of fuel cell/kW | 30 | 21.4232 |

417.9014, that is, under the collaborative optimization control strategy, the minimum equivalent hydrogen consumption of the system is 417.9014 g.
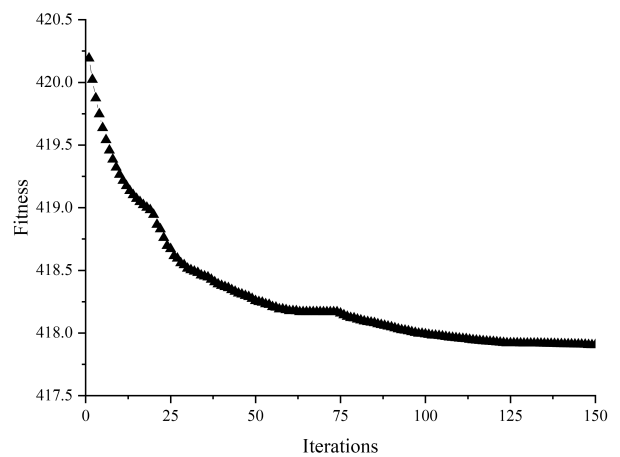


**Fig. 10.** PSO algorithm fitness

Figure 11 shows the output torque and speed of the drive motor under the two strategies and the corresponding motor efficiency. It can be seen from the figure that the average working efficiency of the motor after optimization using the collaborative optimization control strategy is 0.9189, with the highest

*Bull. Pol. Acad. Sci. Tech. Sci.*, vol. 73, no. 2, p. e153232, 2025

7

efficiency reaching 0.93 and the lowest reaching 0.885; the average working efficiency of the motor using the rule control strategy is 0.8996, with the highest efficiency reaching 0.924 and the lowest reaching 0.848. Compared with the rule control strategy, the average working efficiency of the motor is increased by 2.15%.
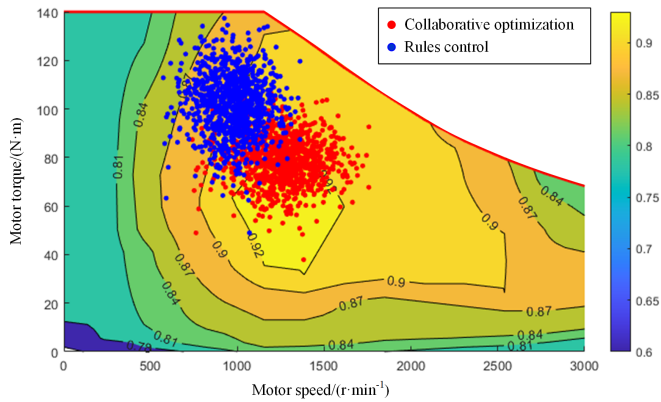


**Fig. 11.** Motor operating point under two control strategies

Figure 12 shows the changes in battery SOC under the two strategies. As can be seen from the figure, the SOC of the power battery using the collaborative optimization control strategy starts to change at the initial value of 0.5, showing an overall downward trend; the SOC of the power battery using the rule control strategy drops to 0.3 at 566 seconds, and then the battery starts to charge, and the battery SOC rises to 0.3381 at the end of the simulation.
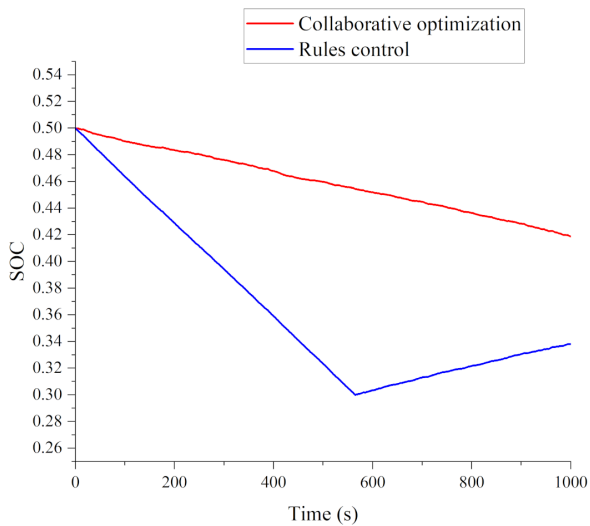


**Fig. 12.** Power battery SOC changes

Figure 13 shows the battery charge and discharge efficiency under the two strategies, where positive values ??represent battery discharge and negative values ??represent battery charge. As can be seen from the figure, the average discharge efficiency of the power battery using the collaborative optimization control strategy is 0.9695, and the average charging efficiency is

0.9878; the average discharge efficiency of the power battery using the rule control strategy is 0.9169, and the average charging efficiency is 0.9706. The charge and discharge efficiency has increased significantly.
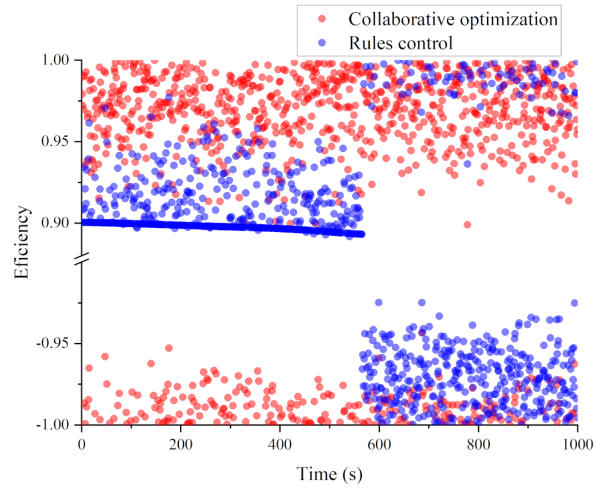


**Fig. 13.** Battery efficiency under two control strategies

Figure 14 shows the discharge efficiency of hydrogen fuel cells under two strategies. As can be seen from the figure, the hydrogen fuel cell fuel using the collaborative optimization control strategy works at an efficiency of around 52.829%, and the average efficiency during the simulation time is 52.8283%; while the fuel cell using rule control has an efficiency of 50.467% to 53.598% in the first 566 seconds, and after 566 seconds, the hydrogen fuel efficiency drops to 49.269%. However, when the battery SOC value drops to the lower limit, the fuel cell efficiency drops sharply to 46.3%, and the average efficiency during the simulation time is 50.456%. Compared with the fuel cell based on rule control, the average efficiency increases by 4.7%.
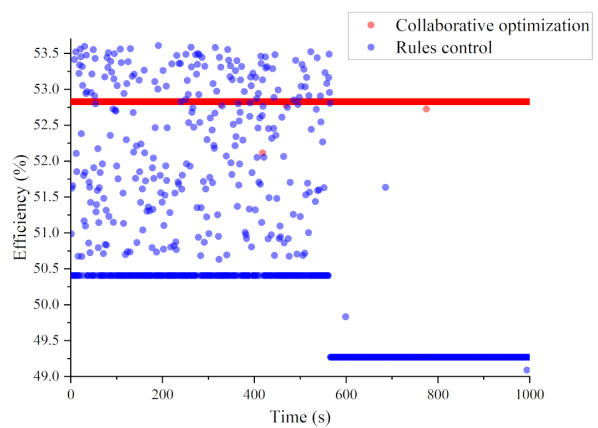


**Fig. 14.** Fuel cell efficiency under two control strategies

Figure 15 shows the efficiency of the power system under the two strategies. The power system includes the hydrogen fuel cell system to the output end of the drive motor. As can be seen from the figure, the efficiency of the power system using the collaborative optimization control strategy is mostly within

8

*Bull. Pol. Acad. Sci. Tech. Sci.*, vol. 73, no. 2, p. e153232, 2025

0.82–0.84, with an average efficiency of 0.8286; the efficiency of the power system using rule control is mostly within 0.78–0.82, with an average efficiency of 0.7927. Compared with the rule control power system, the average efficiency is increased by 4.53%.
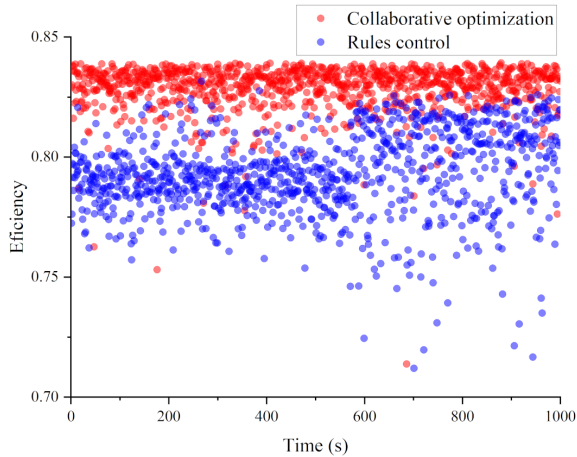


**Fig. 15.** Power system efficiency under two control strategies

Figure 16 shows the equivalent hydrogen consumption under the two control strategies. It can be seen that the equivalent hydrogen consumption of the collaborative optimization control strategy is 419.9014 g; the equivalent hydrogen consumption of the rule control strategy is 455.6369 g. Compared with the rule control, the equivalent hydrogen consumption is reduced by 7.84%. Therefore, the collaborative optimization control strategy proposed in this paper can effectively improve the energy utilization of the whole machine.
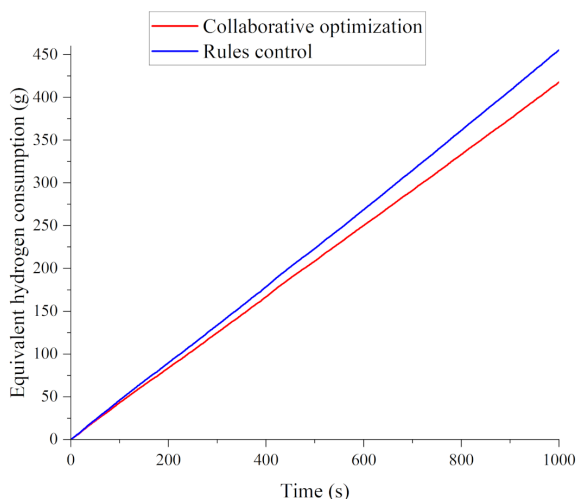


**Fig. 16.** Equivalent hydrogen consumption of the system

## 5. CONCLUSIONS

1. This paper proposes a method for collaborative optimization of the transmission system and energy-saving control strategy parameters, constructs a fuel cell tractor transmission parameter-equivalent hydrogen consumption model, and uses PSO to collaboratively optimize the transmission system and control strategy parameters. The proposed strategy is compared with a rule-based strategy to verify its effectiveness.

2. Under plowing conditions, the equivalent hydrogen consumption of the transmission system and control strategy parameter collaborative optimization control strategy based on the PSO is 419.9014 g, the equivalent hydrogen consumption of the rule control strategy is 455.6369 g, and the equivalent hydrogen consumption is reduced by 7.84%. At the same time, the working efficiency of the fuel cell system and the drive motor is improved, making the hydrogen fuel cell system more dependent on the efficient and stable output of the fuel cell, which is beneficial to control the power battery SOC within a reasonable range.

3. Although the method proposed in this paper greatly reduces the hydrogen consumption of the whole vehicle, achieves lower carbon emissions, and reduces the cost of using hydrogen energy, it may increase the frequency of battery use and deep discharge, resulting in a shortened battery cycle life, requiring more frequent battery replacement, and increasing battery maintenance and replacement costs.

4. Fuel cells have the characteristics of slow dynamic response, and frequent load changes will lead to a reduction in battery life. This paper does not consider its impact on the energy management strategy of hydrogen fuel cell tractors, and further research will be conducted on this basis in the future.

## REFERENCES

[1] L. Xu, J. Zhang, X. Yan, S. Zhao, Y. Wu, and M. Liu, "Review of Research for Agricultural Equipment Electrification Technology," *Trans. Chin. Soc. Agric. Mach.*, vol. 54, no. 09, pp. 1–12, 2023, doi: 10.6041/j.issn.1000-1298.2023.09.001.

[2] M. Liu *et al.*, "Review of Development Process and Research Status of Electric Tractors," *Trans. Chin. Soc. Agric. Mach.*, vol. 53, no. S1, pp. 348–364, 2022, doi: 10.6041/j.issn.1000-1298.2022.S1.039.

[3] V. Martini, F. Mocera, and A. Somà, "Numerical investigation of a fuel cell-powered agricultural tractor," *Energies*, vol. 15, no. 23, p. 8818, 2022, doi: 10.3390/en15238818.

*Bull. Pol. Acad. Sci. Tech. Sci.*, vol. 73, no. 2, p. e153232, 2025

9

[4] V. Olkkonen, A. Lind, E. Rosenberg, and L. Kvalbein, "Electrification of the agricultural sector in Norway in an effort to phase out fossil fuel consumption," *Energy*, vol. 276, p. 127543, 2023, doi: 10.1016/j.energy.2023.127543.

[5] G.P. Moreda, M.A. Muñoz-García, and P. Barreiro, "High voltage electrification of tractor and agricultural machinery – A review," *Energies*, vol. 115, pp. 117–131, 2016, doi: 10.1016/j.enconman.2016.02.018.

[6] J. Teng, Y. Zhang, and X. Ruan, "Some important sciemtific problems for development of renewable and new energy – The only way for development of non-fossil energy," *Prog. Geophys.*, vol. 25, no. 04, pp. 1115–1152, 2010, doi: 10.3969/j.issn.1004-2903.2010.04.001.

[7] J. Carroquino, J.-L. Bernal-Agustín, and R. Dufo-López, "Standalone Renewable Energy and Hydrogen in an Agricultural Context: A Demonstrative Case," *Sustainability*, vol. 11, no. 4, p. 951, 2019, doi: 10.3390/su11040951.

[8] Y. Chen, B. Xie, Y. Du, and E. Mao, "Powertrain parameter matching and optimal design of dual-motor driven electric tractor," *Int. J. Agric. Biol. Eng.*, vol. 12, no. 1, pp. 33–41, 2019, doi: 10.25165/j.ijabe.20191201.3720.

[9] X. Zou *et al.*, "Driving System Parameter Optimization and Energy Control Strategy of Hybrid Electric Buses," *J. Uni. Jinan-Sci. Technol.*, vol. 36, no. 03, pp. 315–321+337, 2022, doi: 10.13349/j.cnki.jdxbn.20211214.007.

[10] B. Li *et al.*, "Optimization method of speed ratio for power-shift transmission of agricultural tractor," *Machines*, vol. 11, no. 4, p. 438, 2023, doi: 10.3390/machines11040438.

[11] X. Li *et al.*, "Optimized Design and Validation of Distributed Drive System for ElectricTractor Based on Multi-island Genetic Algorithm," *Trans. Chin. Soc. Agric. Mach.*, vol. 55, no. 03, pp. 401–411, 2024, doi: 10.6041/j.issn.1000-1298.2024.03.040.

[12] X. Li *et al.*, "Parameters collaborative optimization design and innovation verification approach for fuel cell distributed drive electric tractor," *Energy*, vol. 292, p. 130485, 2024, doi: 10.1016/j.energy.2024.130485.

[13] S. Hou *et al.*, "Reinforcement learning-based energy optimization for a fuel cell electric vehicle," in *2022 4th International Conference on Smart Power & Internet Energy Systems (SPIES)*, 2022, pp. 1928–1933, doi: 10.1109/SPIES55999.2022.10082644.

[14] W. Xu, M. Liu, L. Xu, and S. Zhang, "Energy management strategy of hydrogen fuel cell/battery/ultracapacitor hybrid tractor based on efficiency optimization," *Appl. Sci.*, vol. 13, no. 1, p. 151, 2022, doi: 10.3390/app13010151.

[15] B. Liu, X. Wei, C. Sun, B. Wang, and W. Huo, "A controllable neural network-based method for optimal energy management of fuel cell hybrid electric vehicles," *Int. J. Hydrog. Energy*, vol. 55, pp. 1371–1382, 2024, doi: 10.1016/j.ijhydene.2023.10.215.

[16] X. Lin *et al.*, "Trip distance adaptive equivalent hydrogen consumption minimization strategy for fuel cell electric vehicles integrating driving cycle prediction," *Chin. J. Eng.*, vol. 46, no. 2, pp. 376–384, 2024, doi: 10.13374/j.issn2095-9389.2022.11.22.005.

[17] Z. Chen, R. Liang, F. Qi, and Y. Yan, "Research on Energy Management Method of Fuel Cell Hybrid Power System Based on Improved Equivalent Hydrogen Consumption," *Urban Mass Transit.*, vol. 27, no. 05, pp. 20–24, 2024, doi: 10.16037/j.1007-869x.2024.05.005.

[18] T. Li *et al.*, "Real-time Adaptive Energy Management Strategy for Dual-motor-driven Electric Tractors," *Trans. Chin. Soc. Agric. Mach.*, vol. 51, pp. 530–543, 2020, doi: 10.6041/j.issn.1000-1298.2020.S2.066.

[19] J. Zhang, B. Zhao, X. Yan, M. Liu, L. Xu, and Ch. Shang, "Design and optimization of dual-motor electric tractor drive system based on driving cycles," *Plos One*, vol. 18, no. 16, p. e0286378, 2023, doi: 10.1371/journal.pone.0286378.

[20] G. Pan, Y. Bai, H. Song, Y. Qu, Y. Wang, and X. Wang., "Hydrogen fuel cell power system – development perspectives for hybrid topologies," *Energies*, vol. 16, no. 6, p. 2680, 2023, doi: 10.3390/en16062680.

[21] J. Zhang *et al.*, "Design and optimization of dual-motor electric tractor drive system based on driving cycles," *Trans. Chin. Soc. Agric. Mach.*, vol. 54, pp. 396–406, 2023, doi: 10.6041/j.issn.1000-1298.2023.05.041.

[22] W. Zhou, Y. Zheng, Z. Pan, and Q. Lu, "Review on the battery model and SOC estimation method," *Processes*, vol. 9, no. 9, p. 1685, 2021, doi: 10.3390/pr9091685.

[23] N. Campagna *et al.*, "Battery models for battery powered applications: A comparative study," *Energies*, vol. 13, no. 16, p. 4085, 2020, doi: 10.3390/en13164085.

[24] C. Wang, H. Wang and Y. Tian, "Improved State Machine Strategy Based on Consumption Minimization for Fuel Cell/ Battery/Ultracapacitor Hybrid Electric Vehicles," in *2021 33rd Chinese Control and Decision Conference (CCDC)*, IEEE, 2021, pp. 3778–3783, doi: 10.1109/CCDC52312.2021.9601905.

[25] T. Wang *et al.*, "Fuel Cell Hybrid Power Generation System Equivalent Hydrogen Consumption Instantaneous Optimization Energy Management Method," *Proc. CSEE*, vol. 38, no. 14, pp. 4173–4182, 2018, doi: 10.13334/j.0258-8013.pcsee.171334.

[26] H. Li *et al.*, "A novel equivalent consumption minimization strategy for hybrid electric vehicle powered by fuel cell, battery and supercapacitor," *J. Power Sources*, vol. 395, pp. 262–270, 2018, doi: 10.1016/j.jpowsour.2018.05.078.

[27] X. Li *et al.*, "Drive power allocation strategy for electric tractor based on adaptive multi resolution analysis," *Trans. Chin. Soc. Agric. Mach.*, vol. 39, no. 23, pp. 55–66, 2023, doi: 10.11975/j.issn.1002-6819.202306204.

[28] T. Drugeot *et al.*, "Experimental assessment of proton exchange membrane fuel cell performance degradations during emulated start-up/shut-down phases," *Int. J. Hydrog. Energy*, vol. 48, no. 14, pp. 5630–5642, 2023, doi: 10.1016/j.ijhydene.2022.11.020.

[29] S. Cheng *et al.*, "Investigation and analysis of proton exchange membrane fuel cell dynamic response characteristics on hydrogen consumption of fuel cell vehicle," *Int. J. Hydrog. Energy*, vol. 47, no. 35, pp. 15845–15864, 2022, doi: 10.1016/j.ijhydene.2022.03.063.

[30] B. He and M. Yang, "Optimisation-based energy management of series hybrid vehicles considering transient behaviour," *Int. J. Altern. Propul.*, vol. 1, no. 1, pp. 79–96, 2006, doi: 10.1504/IJAP.2006.010759.

[31] M. Jain, V. Saihjpal, N. Singh, and S.B. Singh, "An overview of variants and advancements of PSO algorithm," *Appl. Sci.*, vol. 12, no. 17, p. 8392, 2022, doi: 10.3390/app12178392.

[32] J. Cai, Q. Li, L. Li, H. Peng, and Y. Yang, "Optimisation-based energy management of series hybrid vehicles considering transient behaviour," *Energy Conv. Manag.*, vol. 53, no. 1, pp. 175–181, 2012, doi: 10.1016/j.enconman.2011.08.023.

[33] N.K. Kulkarni *et al.*, "Particle swarm optimization applications to mechanical engineering – A review," *Mater. Today-Proc.*, vol. 2, no. 4–5, pp. 2631–2639, 2015, doi: 10.1016/j.matpr.2015.07.223.

10

*Bull. Pol. Acad. Sci. Tech. Sci.*, vol. 73, no. 2, p. e153232, 2025